A DFT Study of the Ambiphilic Nature of Arylpalladium Species in Intramolecular Cyclization Reactions

ARTICLE *in* THE JOURNAL OF ORGANIC CHEMISTRY · FEBRUARY 2011

Impact Factor: 4.72 · DOI: 10.1021/jo1020954 · Source: PubMed

3 AUTHORS, INCLUDING:

Israel Fernández
Complutense University of Madrid
188 PUBLICATIONS **3,053** CITATIONS

SEE PROFILE

Miguel A Sierra
Complutense University of Madrid
249 PUBLICATIONS **3,715** CITATIONS

SEE PROFILE

JOC The Journal of Organic Chemistry

ARTICLE

pubs.acs.org/joc

A DFT Study of the Ambiphilic Nature of Arylpalladium Species in Intramolecular Cyclization Reactions

Israel Fernández,*[,†] Daniel Solé,[‡] and Miguel A. Sierra[†]

[†]Departamento de Química Orgánica, Facultad de Química, Universidad Complutense, 28040 Madrid, Spain

[‡]Laboratori de Química Orgànica, Facultat de Farmàcia, Universitat de Barcelona, Av. Joan XXIII s/n, 08028 Barcelona, Spain

Supporting Information

ABSTRACT: The remarkable structure-dependent reactivity observed in the cyclization of (2-haloanilino)-ketones with Pd-catalysts has been studied computationally within the density functional theory framework. The experimental reaction products ratio may be explained through the formation of a common palladaaminocyclobutane intermediate which can undergo a nucleophilic addition reaction and/or an enolate α-arilation process. The evolution of this metallacycle to the final products depends on two factors, the length of the tether joining the amino and the carbonyl groups, and the electronic nature of the substituent directly attached to the nitrogen atom. Thus, shorter chains (2 CH_2) facilitate the nucleophic addition reaction by approximating the reactive aryl and Pd-coordinated carbonyl groups whereas longer chains (3 CH_2) favor the enolate α−arylation procces. For electron-withdrawing groups attached to the aniline nitrogen atom, the nucleophilic addition pathway becomes slightly disfavored, mainly due to the electron-withdrawing effect of the CO_2Me group which avoids the delocation of the LP in the π-system, thus decreasing the nucleophilicity of the reactive arylic carbon atom. In contrast, the enolate α-arylation reaction is facilitated by the CO_2Me group. This is translated into a small computed barrier energy difference of these competitive reaction pathways which should lead to a mixture of reaction products as experimentally found.

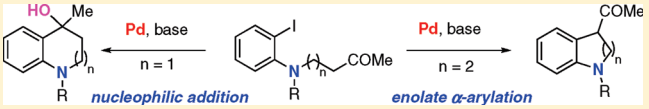

INTRODUCTION

The reactivity of main group organometallics, such as organolithium compounds (RLi) and Grignard reagents (RMgX), is quite straightforward. In these species the R group usually exhibits nucleophilic reactivity and an electrophilic character cannot be induced. In contrast, in organopalladium complexes, switching the usual reactivity from electrophilic to nucleophilic has proven to be quite easy. Thus, although aryl and vinylpalladium complexes are commonly used as electrophiles in C−C bond forming reactions,[1] recent research has demonstrated that they can also react with carbon-heteroatom multiple bonds in a nucleophilic manner. So far, the intramolecular attack of these species has been described on the carbonyl group of aldehydes,[2] ketones,[3] esters,[4] and amides,[5] and on the imino,[6] cyano,[7] and isocyanate[8] groups. Although these addition reactions are still rare, they are growing in popularity because the increased diversity they give to organopalladium compounds is beneficial for organic synthesis. In this context, the direct addition reaction of aryl and vinyl halides to electrophilic partners catalyzed by palladium is a particularly attractive strategy since no extra organometallic reagents are needed.

Few efforts have been made, however, to manipulate the dual character of aryl and vinylpalladium species and selectively promote either the electrophilic or nucleophilic reactivity from the same starting materials.[2f,3d,4,5,9] Solé and co-workers have reported that two different and competitive reaction pathways, involving the enolate arylation and the nucleophilic attack at the carbonyl, can be promoted starting from (2-haloanilino) ketones, which show structure-dependent behavior.[3d] Thus, treatment of γ-(2-iodoanilino) ketone **1** with $PdCl_2(PPh_3)_2$ and Cs_2CO_3

Scheme 1

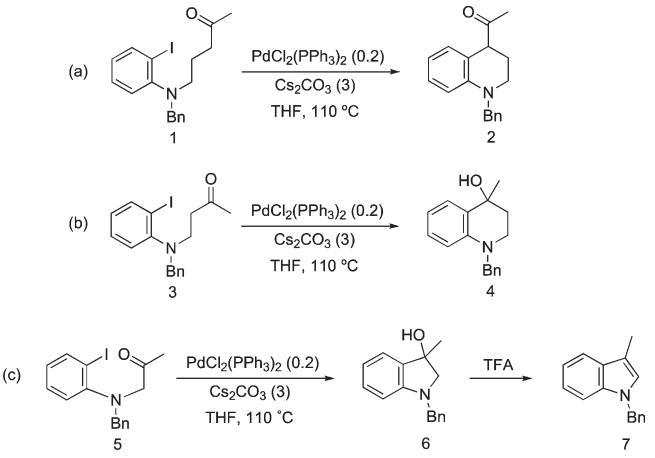

Received: October 22, 2010
Published: February 01, 2011

Scheme 2

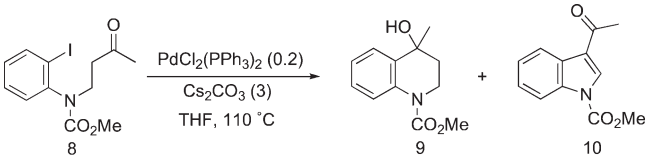

Scheme 3

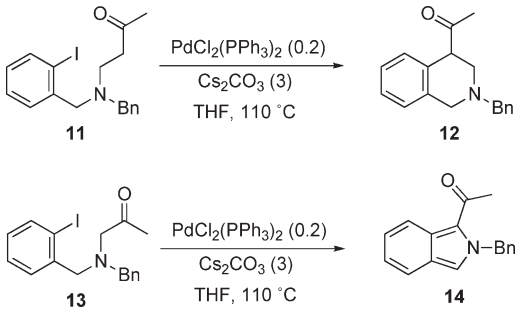

Scheme 4

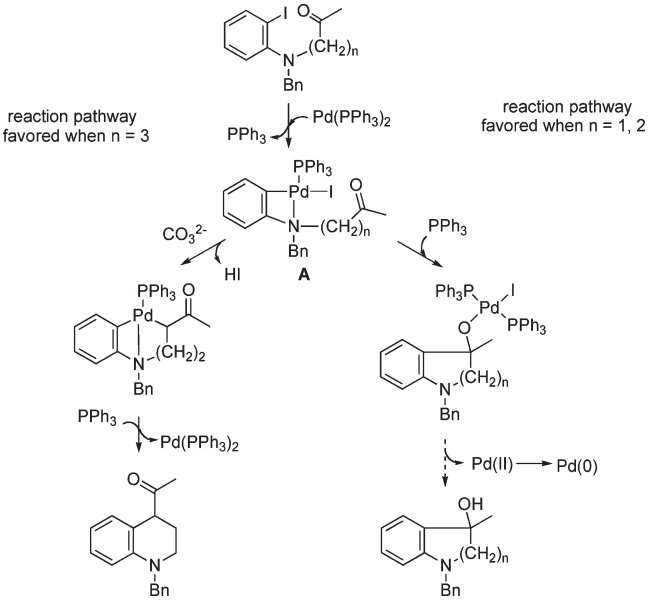

afforded the α-arylation compound **2** (Scheme 1a). In contrast, under the same reaction conditions, *β*-(2-iodoanilino) ketone **3** and α-(2-iodoanilino) ketone **5** exclusively afforded alcohols **4** and **6**, respectively, as a result of the addition of the palladium intermediate to the ketone carbonyl group (Schemes 1b,c).

In the reaction of carbamate **8**, the competition between the nucleophilic addition of the intermediate organopalladium to the carbonyl group or the electrophilic attack of the ketone enolate to this intermediate, resulted in a 1.5:1 mixture of alcohol **9** and indole **10** (Scheme 2). Interestingly, both the intramolecular ketone arylation[10] and the addition of aryl halides to ketones[3b] catalyzed by Pd(0) had been reported for the carbocyclic series. However, the two reactions were not competitive in these cases. Furthermore, *ω*-(2-halobenzylamino) ketones afforded exclusively α-arylation compounds in the presence of a palladium catalysts and base regardless of the structure of the amino ketone (Scheme 3).[3d]

The reaction pathway dichotomy (namely the enolate arylation vs the attack at the carbonyl group) in the Pd-catalyzed reactions of (2-haloanilino) ketones has been rationalized by the intermediacy of four-membered azapalladacycles (A). The different interaction of the metal center with the carbonyl group is chain-length dependent. Shorter carbon tethers (n = 1, 2) will favor the nucleophilic attack of the arylpalladium metallacycle A to the carbonyl group. Longer carbon tethers (n = 3) allow the electrophilic attack of the enolate to the Pd-center (Scheme 4).

Recently, Solé and Serrano have taken advantage of the formation of such putative four-membered azapalladacyclic intermediates to force the nucleophilic attack at functional groups less electrophilic than the ketone carbonyl, such as the alkoxycarbonyl and the carboxamide groups, and to manipulate the divergent reactivity of arylpalladium species.[4a,5,9] Thus, starting from *β*-(2-iodoanilino) esters and *β*-(2-iodoanilino) carboxamides, either the enolate arylation or the nucleophilic substitution at the carbonyl group could be selectively promoted by a subtle modification of the reaction conditions.

The purpose of this paper is to present a computational study of the mechanism of the palladium catalyzed intramolecular coupling reactions of amino-tethered aryl halides and carbonyl groups to achieve a deeper understanding of how the intermediacy of four-membered azapalladacycles modifies the reactivity of the arylpalladium species and exposes their dual character.

RESULTS AND DISCUSSION

We first calculated (B3LYP/def2-SVP level) the reaction path for the transformation of the model compound **1M** (where the benzyl group in compound **1** is replaced by a H-atom) in the presence of the active model catalyst $Pd(PH_3)_2$ to the corresponding α-arylation reaction product **2M**. The theoretically predicted reaction profile (which includes the initial oxidative addition reaction, Figure 1) shows both, in principle, competitive reaction pathways, namely the evolution of palladacycle **16** to complex **18** and the formation of **2M** through enolate palladacycle **22** (Figure 2). The most important interatomic distances of the located saddle points and key intermediates are also displayed in Figures 1 and 2.

(i). Oxidative Addition Reaction. The calculations suggest that the oxidative addition reaction producing **15-*cis*** constitutes the first step of the process. The computed low activation barrier ($\Delta G^{\ddagger}_{298}$ = 9.2 kcal/mol) and exothermicity ($\Delta G_{R,298}$ = −16.9 kcal/mol) of this transformation agrees with previous calculated data for related oxidative addition reactions.[11] Likewise, the main geometrical features of the saddle point **TS1** are similar to those reported for related computed transition states.[11a] Similar to other oxidative addition processes, intermediate **15-*cis*** readily isomerizes to the most stable **15-*trans*** isomer, which lies 2.7 kcal/mol below **15-*cis***.

(ii). Nucleophilic Addition vs α-Arylation Reaction. Complex **15-*trans*** is then transformed into palladacycle **16** (Figure 2). This intermediate is similar to the palladacycle A (n = 3, Scheme 4) that has been experimentally isolated (see above). Formation of the key palladacycle **16** occur stepwise via the acyclic intermediate **19**, formed after decoordination of a PH_3 ligand, through the transition state **TS2** (barrier energy of +9.6 kcal/mol in the gas-phase and +10.6 in tetrahydrofuran solution). The corresponding saddle point which connects **15-*trans*** directly to **16** was not located on the potential energy surface.

dx.doi.org/10.1021/jo1020954 |*J. Org. Chem.* 2011, 76, 1592–1598

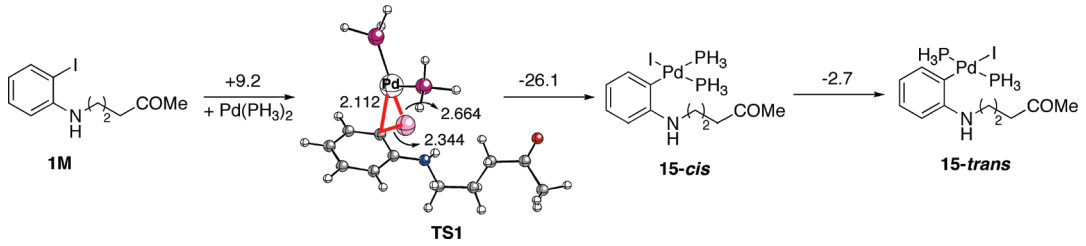

Figure 1. Computed reaction profile for the transformation of **1M** into **15**. Numbers on arrows indicate the corresponding ΔG_{298} energies (in kcal/mol). Bond lengths are given in angstroms. All data have been computed at the B3LYP/def2-SVP level.

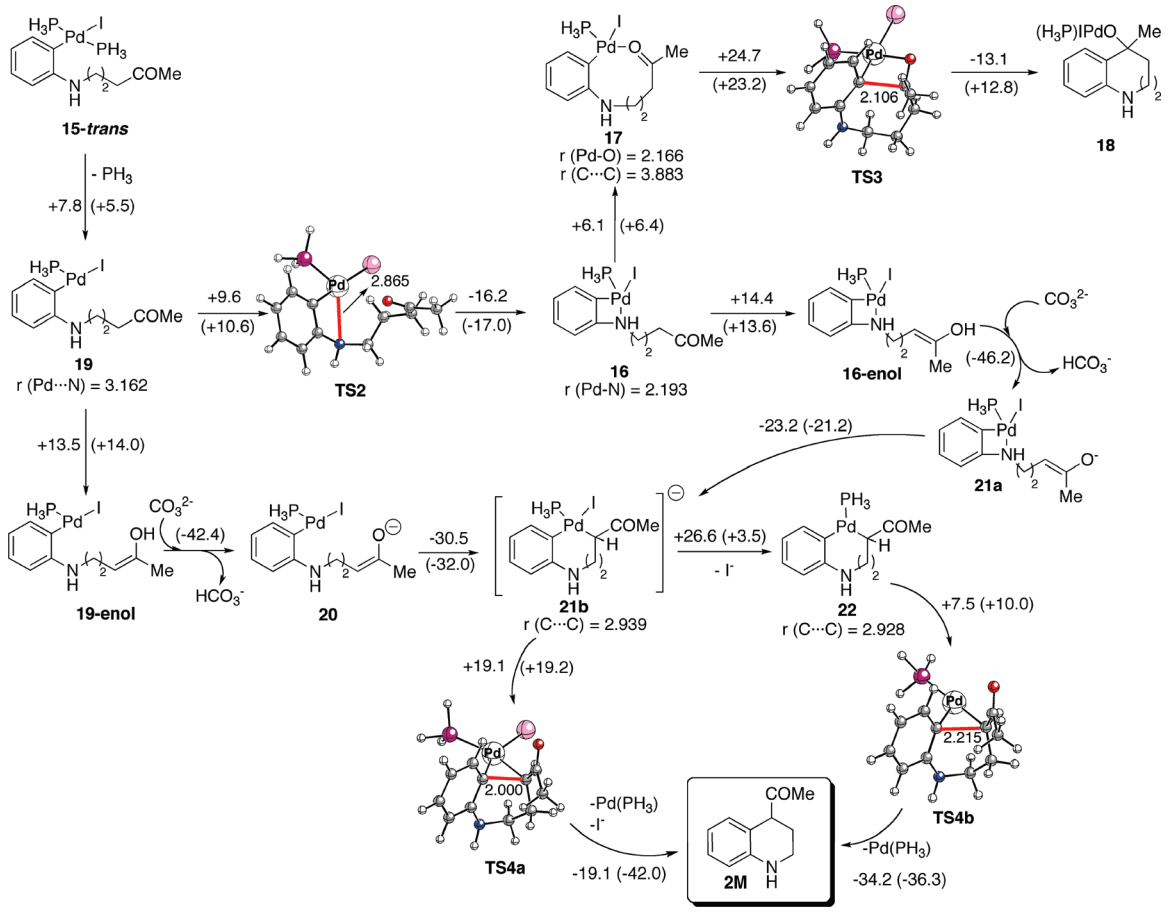

Figure 2. Computed reaction profile for the transformation of **15-*trans*** into **18** and **2M**. Numbers on arrows indicate the corresponding ΔG_{298} energies (in kcal/mol). Numbers in parentheses indicate the corresponding PCM corrected ΔG_{298} energies (in kcal/mol) using tetrahydrofuran as solvent. Bond lengths are given in angstroms. All data have been computed at the B3LYP/def2-SVP level.

Internal ligand interchange of the amino group by the carbonyl group in four-membered palladacycle **16** forms the nine-membered palladacycle **17**. Despite the obvious gain in stability in passing from a four-membered to a nine-membered cycle, this step is slightly endergonic ($\Delta G_{R,298}$ = +6.4 kcal/mol). The endergonic character of this transformation is attributed to the lower donor-ability of the oxygen atom of the carbonyl group compared to the nitrogen atom of the amino group. This fact is reflected in the computed Wiberg indices, which indicate a stronger Pd−N bond in complex **16** compared to the Pd−O bond in compound **17** (bond orders of 0.242 au and 0.184 au, respectively). From compound **17**, intermediate **18**, which would be converted into the corresponding alcohol after hydrolysis, is formed through the transition state **TS3**. This step, which possesses an activation barrier of 24.7 kcal/mol, involves the nucleophilic addition of the aromatic carbon atom attached to the metal center to the carbonyl group. The computed C···C bond length in **TS3** was 2.106 Å (see Figure 2).

The NBO-charges and frontier orbitals of palladacycle **17** nicely agrees with the above description. Thus, whereas the aromatic carbon atom bears a negative charge of −0.25 au, a value of +0.650 au is found for the carbon atom of the carbonyl group. Moreover, the acceptor orbital corresponds to the LUMO (which can be considered as the π^*(C═O) molecular orbital), while the donor orbital corresponds to the HOMO, a delocalized π molecular orbital involving aromatic moiety and the lone pair of the nitrogen atom (Figure 3).

dx.doi.org/10.1021/jo1020954 |J. Org. Chem. 2011, 76, 1592–1598

However, the nucleophilic addition pathway discussed above would lead to alcohols opposite to experimental results when the arylamino group and the carbonyl group are tethered by 3 CH_2-chain. In this case, bicyclic ketones **2** are the experimentally obtained products. The mechanistic branching point occurs by formation of species **21b** upon coordination of the corresponding ketone-enolate (which is produced by base-assisted deprotonation of either metallacycle **16** or acyclic complex **19** via the corresponding enols).[12] Interestingly, the formation of the bicyclic ketone **2M** from the anionic complex **21b** via transition state **TS4a** occurs with a computed barrier energy of $\Delta G‡_{298}$ = 19.1 kcal/mol. This transformation is kinetically favored respect to the nucleophilic addition in **17**, which would form the alcohol derived from **18**, involving the saddle point **TS3** ($\Delta\Delta G‡_{298}$ = 5.6 kcal/mol in the gas-phase and 4.0 kcal/mol in solution). Therefore, the formation of ketone **2M** is favored over the alcohol produced from **18**. We also computed the analogous process starting from **22**, which produces **2M** through **TS4b** with an activation barrier of only $\Delta G‡_{298}$ = 7.5 kcal/mol. The dissociation of the iodide ligand in **21b** is highly endergonic ($\Delta G_{R,298}$ = +26.6 kcal/mol) rendering this process very unlikely. However, when solvent effects are considered, the dissociation is only slightly endergonic ($\Delta G_{R,298}$ = +3.5 kcal/mol) making the process feasible and clearly favored over the nucleophilic addition pathway ($\Delta\Delta G‡_{298}$ = 9.7 kcal/mol including the iodine ligand dissociation).

Thus, it can be concluded that the selectivity of the reaction is mainly determined by the difference of the activation barriers of the nucleophilic addition of the aryl group to the carbonyl group in intermediate **17**, and the enolate α-arylation processes in intermediates **21b** or **22**. Furthermore, in view of the computed frontier orbitals and NBO-charges of palladacycle **21b**, this enolate α-arylation process involves the nucleophilic addition of the aromatic carbon atom (HOMO) to the carbon atom placed in α-position to the carbonyl group (the LUMO is mainly located in the π^* C═C(-O) molecular orbital, Figure 4).

To check our proposed reaction mechanism, the corresponding reaction profile of **3M**, a model compound of **3** which experimentally leads to exclusive formation of alcohol **4M** at the expenses of ketone **31**, was computed. It is quite remarkable that the shortening of the tether joining the amino and the carbonyl group by a CH_2 completely switches the reactivity. Similarly to **1M**, **3M** is converted into metallacycle **24** after an oxidative addition process followed by *cis*- to *trans*- isomerization reaction. The corresponding reaction barriers and energies are analogous to those computed for the **1M** species (Figure 5).

Palladacycle **24**, formed from complex **27** via transition state **TS2′** (activation barrier of 6.5 kcal/mol in solution), is readily converted into the eight-membered palladacycle **25** in a slightly endergonic process or even slightly exergonic when solvent effects are considered (Figure 6). The formation of complex **25** from **24** is therefore favored compared to the formation of its counterpart **17** from complex **16**. Interestingly, the nucleophilic addition process forming **26** via **TS3′** occurs with an activation barrier of 17.5 kcal/mol in the gas-phase (17.3 kcal/mol in tetrahydrofuran), that is 7.2 kcal/mol (5.9 kcal/mol in solution) lower than the respective process involving **1M** as starting reactant (Figure 2). The origins of this dramatic reduction of the barrier energy can be mainly ascribed to the shorther length between the reactive aryl and CO centers in **25** (3.584.Å) compared to **17** (3.883 Å). In contrast, the enolate α-arylation reaction product, namely the experimentally nonobserved bicyclic ketone **31** formed via **TS4a′**, possesses an activation barrier of 22.5 kcal/mol (21.3 kcal/mol in solution), that is 3.4 kcal/mol (2.1 kcal/mol in solution) higher than the respective process involving **1M** as starting reactant, and strikingly, 5.0 kcal/mol (4.0 kcal/mol in THF) higher than the step connecting **25** and **26**. This inversion in the computed barrier energies justifies the observed inversion in the selectivity of the process using compounds **1** and **3** and therefore, provides further support to the proposed reaction profile given by

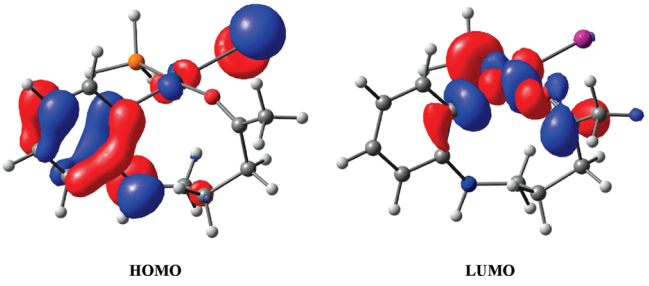

Figure 3. Frontier molecular orbitals of palladacycle **17** (isosurface value of 0.05 au).

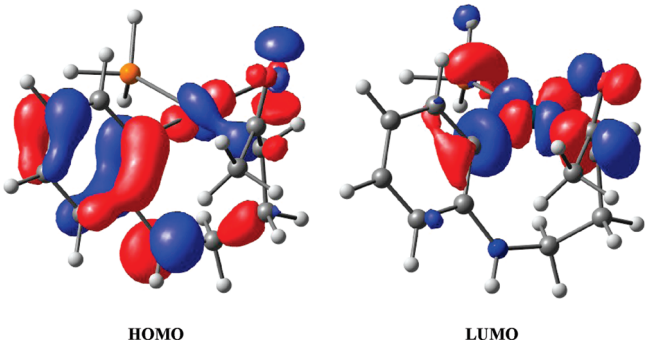

Figure 4. Frontier molecular orbitals of palladacycle **21b** (isosurface value of 0.05 au).

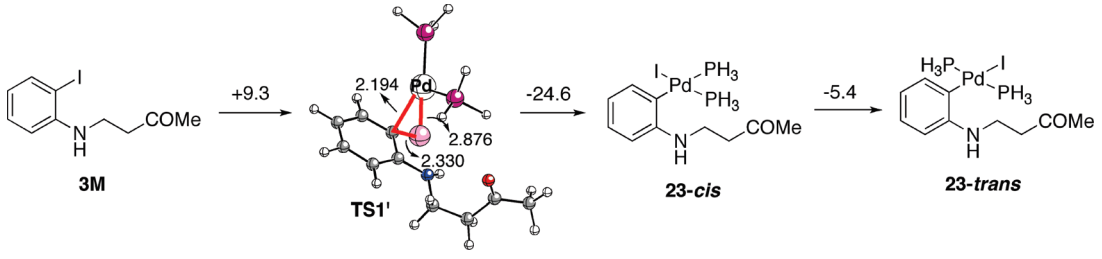

Figure 5. Computed reaction profile for the transformation of **3M** into **23**. Numbers on arrows indicate the corresponding ΔG_{298} energies (in kcal/mol). Bond lengths are given in angstroms. All data have been computed at the B3LYP/def2-SVP level.

dx.doi.org/10.1021/jo1020954 |*J. Org. Chem.* 2011, 76, 1592–1598

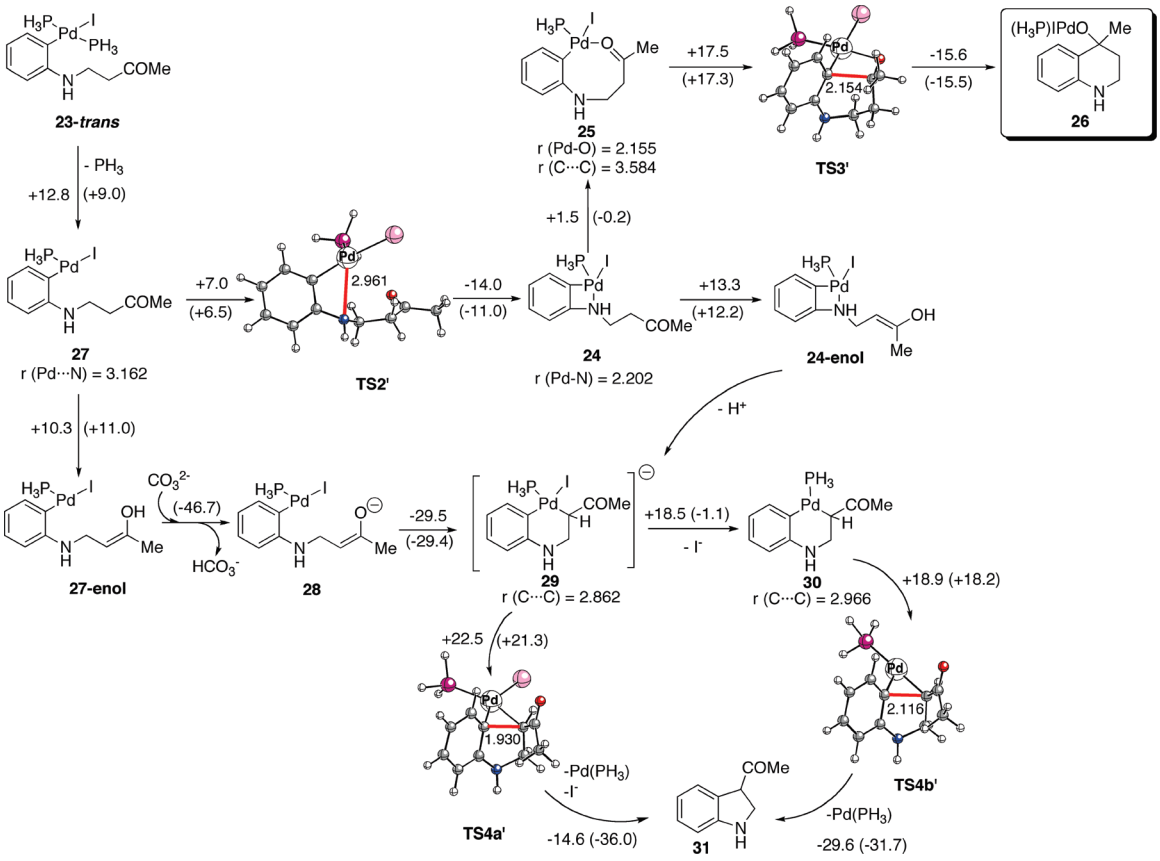

Figure 6. Computed reaction profile for the transformation of **23-*trans*** into **26** and **31**. Numbers on arrows indicate the corresponding ΔG_{298} energies (in kcal/mol). Numbers in parentheses indicate the corresponding PCM corrected ΔG_{298} energies (in kcal/mol) using tetrahydrofuran as solvent. Bond lengths are given in angstroms. All data have been computed at the B3LYP/def2-SVP level.

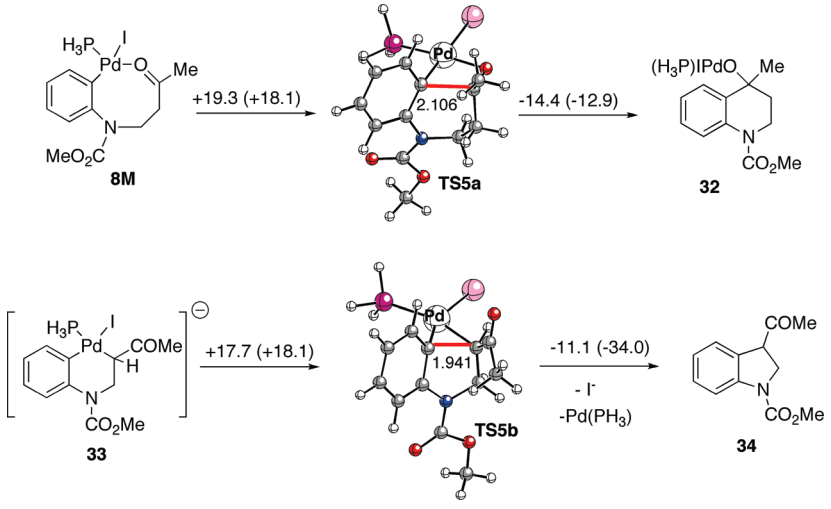

Figure 7. Computed reaction profile for the **8M** → **32** and **33** → **34** transformations. Numbers on arrows indicate the corresponding ΔG_{298} energies (in kcal/mol). Numbers in parentheses indicate the corresponding PCM corrected ΔG_{298} energies (in kcal/mol) using tetrahydrofuran as solvent. Bond lengths are given in angstroms. All data have been computed at the B3LYP/def2-SVP level.

the calculations. We also computed the enolate α-arylation reaction from compound **30**, formed after dissociation of the iodide ligand. Similarly to the reaction profile of compound **1M**, the activation barrier involving **TS4b′** is lower than that involving **TS4a′**. However, this step also proceeds with a higher barrier energy than the nucleophilic addition process.

(iii). Effect of a CO_2Me Group Attached to the Nitrogen Atom. The effect of the replacement of the *N*-benzyl group in **3** to the *N*−CO_2Me group in **8** was addressed next. The experimental result indicates that the reaction of carbamate **8** produces the nucleophilic and enolate α-arylation competition and therefore a 1.5:1 mixture of alcohol **9** and indole **10** is found

dx.doi.org/10.1021/jo1020954 |*J. Org. Chem.* 2011, 76, 1592–1598

(Scheme 2). Our calculations indicate that the introduction of the CO_2Me group increases the activation barrier of the nucleophilic addition (Figure 7). Thus, the process involving **TS5a** is more difficult than the analogous process involving **TS3′** ($\Delta\Delta G^{\ddagger}_{298}$ = 1.8 kcal/mol in the gas-phase and 0.8 kcal/mol in tetrahydrofuran solution). According to the molecular orbitals depited in Figure 2, the HOMO exhibits a significant contribution of the LP of the nitrogen atom. Therefore, this increase in the energy barrier is mainly due to the electron-withdrawing effect of the CO_2Me group which avoids the delocation of the LP in the π-system decreasing the nucleophilicity of the reactive arylic carbon atom. This is clearly reflected in the computed lower NBO-charge of this carbon atom (−0.245 au in **25** and −0.208 au in **8M**) and also in the lower N−C Wiberg-bond order (1.09 au in **25** and 0.94 au in **8M**).

Interestingly, the enolate α-arylation reaction from anionic complex **33** is kinetically easier than from the analogous complex **29** (activation barrier 4.8 kcal/mol lower in the gas-phase and 3.2 kcal/mol in solution). Therefore, the CO_2Me group facilitates the latter transformation. Thus, the difference in the barrier energies of nucleophilic addition and α-arylation processes is reduced from 5.0 kcal/mol (see Figure 6) to only 1.6 kcal/mol when the hydrogen group in **3M** is replaced to the CO_2Me group in **8M**. This computed small value should translate into a mixture of the reaction products as it was experimentally found. Moreover, when solvents effects are taken into account, no differences were found in the corresponding activation barriers which nicely agrees with the experimental result.

CONCLUSIONS

From the computational-DFT study reported in this paper, the following conclusions can be drawn: (i) the formation of a common palladaaminocyclobutane intermediate, which can undergo a nucleophilic addition reaction and/or an enolate α-arylation process, is the key point to explain the experimentally observed reaction products ratio. (ii) The evolution of this metallacycle to the final products depends mainly on two factors, the length of the tether joining the amino and the carbonyl groups, and the electronic nature of the substituent directly attached to the nitrogen atom. (iii) While shorter chains (2 CH_2) facilitates the nucleophic addition reaction by approximating the reactive aryl and coordinated carbonyl groups, longer chains (3 CH_2) favor the enolate α−arylation procces. (iv) Electron-withdrawing groups directly attached to the aniline nitrogen atom disfavor the nucleophilic addition process. This is mainly due to the electron-withdrawing effect of the CO_2Me group, which avoids the delocation of the LP in the π-system, thus decreasing the nucleophilicity of the reactive arylic carbon atom. (v) In contrast, the enolate α-arylation reaction is facilitated by the CO_2Me group which is translated into a small or negligible barrier energy difference of these competitive reaction pathways. This leads to a mixture of reaction products, which is in nice agreement with the experimental findings.

COMPUTATIONAL DETAILS

All the calculations reported in this paper were obtained with the GAUSSIAN 03 suite of programs.[13] Electron correlation was partially taken into account using the hybrid functional usually denoted as B3LYP[14] using the double-ζ quality plus polarization def2-SVP basis set[15] for all atoms (this basis sets include effective core potentials, ECPs, for palladium and iodine atoms). Reactants and products were characterized by frequency calculations,[16] and have positive definite Hessian matrices. Transition structures (TS′s) show only one negative eigenvalue in their diagonalized force constant matrices, and their associated eigenvectors were confirmed to correspond to the motion along the reaction coordinate under consideration using the Intrinsic Reaction Coordinate (IRC) method.[17] The Wiberg bond indices[18] *Bi* and atomic charges were computed using the natural bond orbital (NBO)[19] method. Solvents effects were taken into account using the Polarizable Continuum Model (PCM).[20] Single point calculations (PCM-B3LYP/def2-SVP) on the gas-phase optimized geometries were performed to estimate the change in the Gibbs energies in the presence of tetrahydrofuran as solvent.

ASSOCIATED CONTENT

Supporting Information. Cartesian coordinates (Å) and total energies (au, noncorrected zero-point vibrational energies included) of all the stationary points discussed in the text and complete ref 13. This material is available free of charge via the Internet at http://pubs.acs.org.

AUTHOR INFORMATION

Corresponding Author
*E-mail: israel@quim.ucm.es.

ACKNOWLEDGMENT

Support for this work under grants CTQ2007-67730-C02-01/BQU, CSD2007-0006 (Programa Consolider-Ingenio 2010) from the MEC (Spain), P2009/PPQ1634-AVANCAT from the CAM, and CTQ2009-07175 from the MEC (Spain) is gratefully acknowledged. Dr. I. Fernández is a Ramón y Cajal fellow.

REFERENCES

(1) Negishi, E., Ed. *Handbook of Organopalladium Chemistry for Organic Synthesis*; Wiley-VCH: New York, 2002; Vols. I and II.

(2) (a) Larock, R. C.; Doty, M. J.; Cacchi, S. *J. Org. Chem.* **1993**, *58*, 4579–4583. (b) Gevorgyan, V.; Quan, L. G.; Yamamoto, Y. *Tetrahedron Lett.* **1999**, *40*, 4089–4092. (c) Zhao, L.; Lu, X. *Angew. Chem., Int. Ed.* **2002**, *41*, 4343–4345. (d) Vicente, J.; Abad, J.-A.; López-Peláez, B.; Martínez-Viviente, E. *Organometallics* **2002**, *21*, 58–67. (e) Yang, M.; Zhang, X.; Lu, X. *Org. Lett.* **2007**, *9*, 5131–5133. (f) Zhao, Y.-B.; Mariampillai, B.; Candito, D. A.; Laleu, B.; Li, M.; Lautens, M. *Angew. Chem., Int. Ed.* **2009**, *48*, 1849–1852. (g) Álvarez-Bercedo, P.; Flores-Gaspar, A.; Correa, A.; Martin, R. *J. Am. Chem. Soc.* **2010**, *132*, 466–467.

(3) (a) Quan, L. G.; Gevorgyan, V.; Yamamoto, Y. *J. Am. Chem. Soc.* **1999**, *121*, 3545–3546. (b) Quan, L. G.; Lamrani, M.; Yamamoto, Y. *J. Am. Chem. Soc.* **2000**, *122*, 4827–4828. (c) Solé, D.; Vallverdú, L.; Peidró, E.; Bonjoch, J. *Chem. Commun.* **2001**, 1888–1889. (d) Solé, D.; Vallverdú, L.; Solans, X.; Font-Bardia, M.; Bonjoch, J. *J. Am. Chem. Soc.* **2003**, *125*, 1587–1594. (e) Liu, G.; Lu, X. *J. Am. Chem. Soc.* **2006**, *128*, 16504–16505. (f) Song, J.; Shen, Q.; Xu, F.; Lu, X. *Org. Lett.* **2007**, *9*, 2947–2950. (g) Liu, G.; Lu, X. *Adv. Synth. Catal.* **2007**, *349*, 2247–2252. (h) Liu, G.; Lu, X. *Tetrahedron* **2008**, *64*, 7324–7330. (i) Jia, Y.-X.; Katayev, D.; Kündig, E. P. *Chem. Commun.* **2010**, 130–132. See also ref2c,2d,2f.

(4) (a) Solé, D.; Serrano, O. *Angew. Chem., Int. Ed.* **2007**, *46*, 7270–7272.(b) See also ref 2f.

(5) Solé, D.; Serrano, O. *J. Org. Chem.* **2008**, *73*, 9372–9378.

(6) (a) Takeda, A.; Kamijo, S.; Yamamoto, Y. *J. Am. Chem. Soc.* **2000**, *122*, 5662–5663. (b) Ohno, H.; Aso, A.; Kadoh, Y.; Fujii, N.; Tanaka, T. *Angew. Chem., Int. Ed.* **2007**, *46*, 6325–6328.

(7) (a) Yang, C.-C.; Sun, P.-J.; Fang, J.-M. *J. Chem. Soc., Chem. Commun.* **1994**, 2629–2630. (b) Larock, R. C.; Tian, Q.; Pletnev, A. A. *J. Am. Chem. Soc.* **1999**, *121*, 3238–3239. (c) Pletnev, A. A.; Tian, Q.; Larock, R. C. *J. Org. Chem.* **2002**, *67*, 9276–9287. (d) Pletnev, A. A.; Larock, R. C. *J. Org. Chem.* **2002**, *67*, 9428–9438. (e) Tian, Q.; Pletnev, A. A.; Larock, R. C. *J. Org. Chem.* **2003**, *68*, 339–347. (f) Zhou, C.; Larock, R. C. *J. Am. Chem. Soc.* **2004**, *126*, 2302–2303. (g) Zhou, C.; Larock, R. C. *J. Org. Chem.* **2006**, *71*, 3551–3558.

(8) Kamijo, S.; Sasaki, Y.; Kanazawa, C.; Schüsseler, T.; Yamamoto, Y. *Angew. Chem., Int. Ed.* **2005**, *44*, 7718–7721.

(9) Solé, D.; Serrano, O. *J. Org. Chem.* **2008**, *73*, 2476–2479.

(10) Muratake, H.; Natsume, M. *Tetrahedron Lett.* **1997**, *38*, 7581–7582.

(11) (a) Braga, A. C. A.; Ujaque, G.; Maseras, F. *Organometallics* **2006**, *25*, 3647. See also: (b) Sundermann, A.; Uzan, O.; Martin, J. M. L. *Chem.—Eur. J.* **2001**, *7*, 1703. (c) Goossen, L. J.; Koley, D.; Hermann, H.; Thiel, W. *Organometallics* **2005**, *24*, 2398. (d) Sakaki, S.; Mizoe, N.; Musashi, Y.; Biswas, B.; Sugimoto, M. *J. Phys. Chem. A* **1998**, *102*, 8027. (e) Albert, K.; Gisdakis, P.; Rösch, N. *Organometallics* **1998**, *17*, 1608.

(12) Regarding the interaction between the enolate and Pd center, as, for example, for complex **21a**, there is no interaction between the double bond of the enolate (bond length Pd−C: 5.396 Å) or the oxygen atom of the carbonyl group (bond length Pd−O: 5.912 Å). Moreover, the corresponding Wiberg indices are practically negligible.

(13) Gaussian 03, Revision D.01: Frisch, M. J. et al. Gaussian, Inc., Wallingford, CT, 2004.

(14) (a) Becke, A. D. *J. Chem. Phys.* **1993**, *98*, 5648. (b) Lee, C.; Yang, W.; Parr, R. G. *Phys. Rev. B* **1998**, *37*, 785. (c) Vosko, S. H.; Wilk, L.; Nusair, M. *Can. J. Phys.* **1980**, *58*, 1200.

(15) Weigend, F.; Ahlrichs, R. *Phys. Chem. Chem. Phys.* **2005**, *7*, 3297.

(16) McIver, J. W.; Komornicki, A. K. *J. Am. Chem. Soc.* **1972**, *94*, 2625.

(17) González, C.; Schlegel, H. B. *J. Phys. Chem.* **1990**, *94*, 5523.

(18) Wiberg, K. B. *Tetrahedron* **1968**, *24*, 1083.

(19) (a) Foster, J. P.; Weinhold, F. *J. Am. Chem. Soc.* **1980**, *102*, 7211. (b) Reed, A. E.; Weinhold, F. J. *J. Chem. Phys.* **1985**, *83*, 1736. (c) Reed, A. E.; Weinstock, R. B.; Weinhold, F. *J. Chem. Phys.* **1985**, *83*, 735. (d) Reed, A. E.; Curtiss, L. A.; Weinhold, F. *Chem. Rev.* **1988**, *88*, 899.

(20) (a) Miertuš, S.; Scrocco, E.; Tomasi, J. *Chem. Phys.* **1981**, *55*, 117. (b) Pascual-Ahuir, J. L.; Silla, E.; Tuñón, I. *J. Comput. Chem.* **1994**, *15*, 1127. (c) Barone, V.; Cossi, M. *J. Phys. Chem. A* **1998**, *102*, 1995.